NASA TECHNICAL NOTE

NASA TN D-7079

NASA TN D-7079

DIFFUSIONAL CREEP AND CREEP DEGRADATION IN THE DISPERSION-STRENGTHENED ALLOY TD-NiCr

by John D. Whittenberger

Lewis Research Center
Cleveland, Ohio 44135

NATIONAL AERONAUTICS AND SPACE ADMINISTRATION • WASHINGTON, D. C. • DECEMBER 1972

1. Report No.	2. Government Accession No.	3. Recipient's Catalog No.
NASA TN D-7079		

4. Title and Subtitle	5. Report Date
DIFFUSIONAL CREEP AND CREEP DEGRADATION IN THE DISPERSION-STRENGTHENED ALLOY TD-NiCr	December 1972
	6. Performing Organization Code

7. Author(s)	8. Performing Organization Report No.
John D. Whittenberger	E-7080
	10. Work Unit No. 502-21
9. Performing Organization Name and Address	11. Contract or Grant No.
Lewis Research Center National Aeronautics and Space Administration Cleveland, Ohio 44135	13. Type of Report and Period Covered
	Technical Note
12. Sponsoring Agency Name and Address	14. Sponsoring Agency Code
National Aeronautics and Space Administration Washington, D.C. 20546	

15. Supplementary Notes

16. Abstract

Dispersoid-free regions were observed in TD-NiCr (Ni-20Cr-2ThO_2) after slow strain rate testing in air from 1145 to 1590 K. Formation of the dispersoid-free regions appears to be the result of diffusional creep. The net effect of this creep is the degradation of TD-NiCr to a duplex microstructure. Degradation is further enhanced by the formation of voids and intergranular oxidation in the thoria-free regions. These regions apparently provided sites for void formation and oxide growth since the strength and oxidation resistance of Ni-20Cr is much less than Ni-20Cr-2ThO_2. This localized oxidation does not appear to reduce the static load bearing capacity of TD-NiCr since long stress-rupture lives were observed even with heavily oxidized microstructures. But this oxidation does significantly reduce the ductility and impact resistance of the material. Dispersoid-free bands and voids were also observed for two other dispersion-strengthened alloys, TD-NiCrAl and IN-853. Thus, it appears that diffusional creep is characteristic of dispersion-strengthened alloys and can play a major role in the creep degradation of these materials.

17. Key Words (Suggested by Author(s))	18. Distribution Statement
Dispersion-strengthened alloys Diffusional creep Creep Nickel-base alloys	Unclassified - unlimited

19. Security Classif. (of this report)	20. Security Classif. (of this page)	21. No. of Pages	22. Price*
Unclassified	Unclassified	30	$3.00

* For sale by the National Technical Information Service, Springfield, Virginia 22151

CONTENTS

DIFFUSIONAL CREEP AND CREEP DEGRADATION IN THE DISPERSION-STRENGTHENED ALLOY TD-NiCr

by John D. Whittenberger

Lewis Research Center

SUMMARY

Dispersoid-free regions were observed in the dispersion-strengthened alloy TD-NiCr (Ni-20Cr-2ThO_2) after slow strain rate testing (stress rupture, creep, and fatigue) in air from 1145 to 1590 K. Formation of the dispersoid-free regions appears to be the result of diffusional creep. The net effect of creep in TD-NiCr is the degradation of the alloy to a duplex microstructure.

Creep degradation of TD-NiCr is further enhanced by the formation of voids and intergranular oxidation in the dispersoid-free bands. Void formation was observed after as little as 0.13 percent creep deformation at 1255 K. The dispersoid-free regions apparently provide sites for void formation and oxide growth since the strength and oxidation resistance of Ni-20Cr is much less than Ni-20Cr-2ThO_2. This localized oxidation does not appear to reduce the static load bearing capacity of TD-NiCr since long stress rupture lives were observed even with heavily oxidized microstructures. But this oxidation does significantly reduce the ductility and impact resistance of the material.

Dispersoid-free bands and voids also were observed for two other dispersion-strengthened alloys, TD-NiCrAl (Ni-16Cr-4Al-2ThO_2) and IN-853 (Ni-20Cr-2.5Ti-1.5Al-1.3Y_2O_3). Thus, it appears that diffusional creep is characteristic of dispersion-strengthened alloys and can play a major role in the creep degradation of these materials.

INTRODUCTION

Considerable emphasis has been placed on the development of high temperature, high creep strength alloys through dispersion-strengthening techniques. In general, these alloys are composed of hard nonmetallic particles (oxides, carbides, etc.) embeded in a metallic matrix. The particles contribute both directly and indirectly to the strength of such alloys (refs. 1 to 3). Direct strengthening is the result of particles

acting as obstacles to dislocation motion, and indirect strengthening is the result of the particles stabilizing a dislocation substructure and grain structure. Because of these types of strengthening, dispersion-strengthened alloys should be ideal candidates for diffusional (Nabarro-Herring or Coble) creep (refs. 4 to 6). (See appendix for general discussion of diffusional creep.)

Diffusional creep, if it is a characteristic of dispersion-strengthened alloys, can reduce the effectiveness of the dispersoid as a strengthening agent. This is schematically illustrated in figure 1. In diffusional creep, mass flow to grain boundaries which

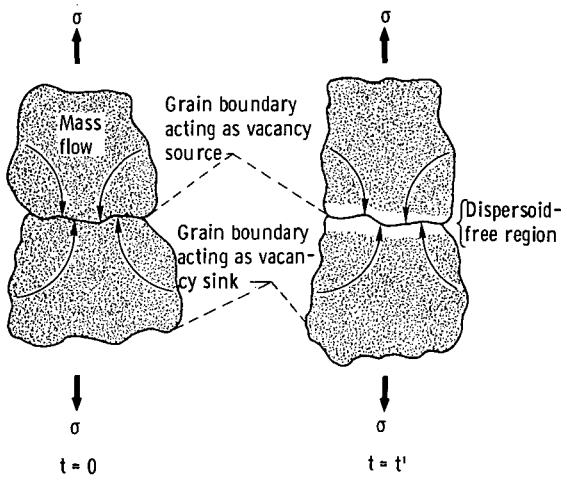

Figure 1. - Schematic representation of diffusional creep in a dispersion-strengthened alloy.

act as vacancy sources (i.e., grain boundaries which tend to be normal to the applied tensile axis) results in the formation of dispersoid-free zones at these grain boundaries. During exposure to stress and temperature, the alloy would be degraded from a system containing a uniform dispersion to a duplex system where bands of weak dispersoid-free alloy separate regions of strong dispersion-strengthened material. Ultimately, the alloy should fail by the formation and growth of voids in the weaker dispersoid-free bands.

Several observations of this type of behavior have been reported for various materials containing a dispersed second phase. For example, diffusional creep has been observed during high temperature ($T/T_M \approx 0.8$) creep and slow tension testing of hydrided Mg-Zr alloys (refs. 7 to 10). The alloys tested were nominally Mg-0.5Zr, which formed a homogeneous dispersion of ZrH_2 particles when annealed in hydrogen. During testing, ZrH_2-free regions were formed around grain boundaries which tended to be normal to the applied tensile stress. This observation was interpreted as evidence that diffusional creep occurred. Also, Karim, et al. (refs. 8 and 9) observed that voids

formed in the precipitate-free zones and that these led to failure of the specimen. Additionally, several studies (refs. 11 and 12) of high temperature ($T/T_M \approx 0.7$) creep in γ' precipitation-strengthened Ni-base superalloys indicate that diffusional creep may be an active creep mechanism in these alloys. In these studies, γ'-free regions were observed around grain boundaries which generally lie at right angles to the applied tensile stress.

Thoriated Ni-base alloys are, to date, the best examples of successful dispersion-strengthened systems for use at elevated temperatures. These alloys are intended for use in situations where high temperature creep strength is required. While considerable high temperature testing of thoriated Ni-base alloys has been conducted (e.g., refs. 13 to 16), diffusional creep has not been reported for these materials. However, recent results (ref. 17) of room temperature tensile tests of TD-NiCr (Ni-20Cr-2ThO_2) specimens which had been previously creep tested at 1365 K to various strain levels revealed that the tensile properties were reduced by the effects of even small creep strains (fig. 2). Such reductions would be expected if TD-NiCr underwent diffusional creep since the majority of the tensile deformation would be confined to the weaker nonthoriated regions that had formed during the previous creep deformation.

This study examined the microstructure of dispersion-strengthened Ni-base alloys after slow strain rate, high temperature testing for evidence of diffusional creep. Emphasis was placed on evaluation of stress-rupture tested TD-NiCr because of the availability of tested specimens. But several specimens of TD-NiCr which had been

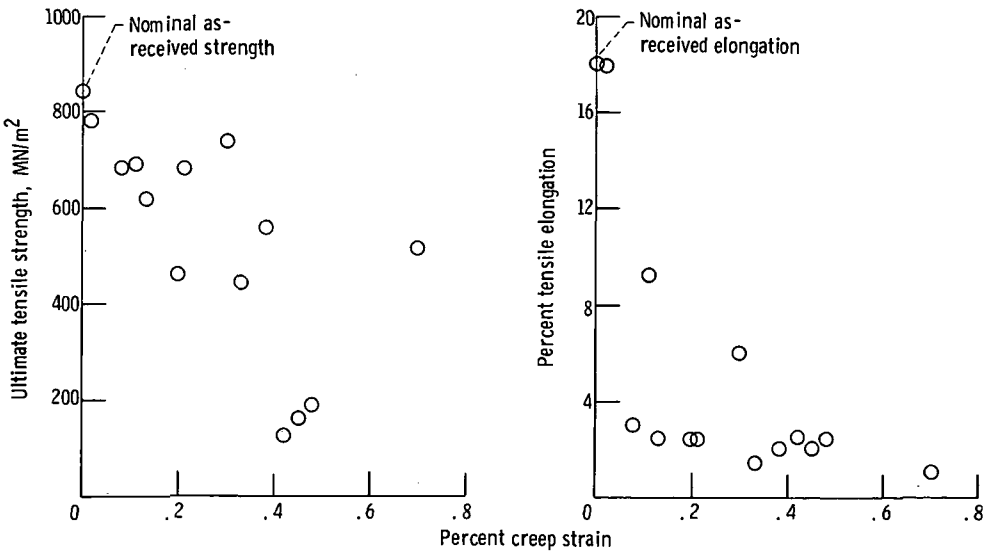

(a) Ultimate tensile strength.

(b) Tensile elongation.

Figure 2. - Effects of creep strain on subsequent room temperature tensile properties of TD-NiCr sheet (0.025 to 0.075 cm) after creep testing at 1365 K for 100 hours at various stress levels. (From ref. 17.)

creep or fatigue tested and a few specimens of other dispersion-strengthened alloys (TD-NiCrAl and IN-853) which had been creep or stress rupture tested were included.

EXPERIMENT

The materials evaluated in this study are described in table I. The majority of the 0.025- and 0.051-centimeter-thick TD-NiCr sheet specimens were tested in air at

TABLE I. - DISPERSION-STRENGTHENED ALLOYS EVALUATED

Alloy	Heat	Composition	Form	Thickness, cm
TD-NiCr	3636	Ni-20.2Cr-0.02C-0.002S-2.2ThO_2	Sheet	0.051
	3637	Ni-19.8Cr-0.02C-0.002S-2.1ThO_2		.025
	3697	Ni-20.1Cr-0.02C-0.006S-2.1ThO_2		.025
	3090	Ni-20.2Cr-0.03C-0.004S-2.1ThO_2		.160
	----	Ni-21.1Cr-0.02C-0.007S-2.3ThO_2		.051
	----	Ni-19.4Cr-0.003C-0.001S-2.4ThO_2		.049
TD-NiCrAl	3774	Ni-16Cr-3.9Al-2ThO_2		.025
IN-853	----	Ni-20Cr-2.5Ti-0.15Al-0.2Fe-0.05C-0.07Zr-0.007B-1.3Y_2O_3	Bar	1.6 diameter (0.63 diam test section)

Metcut Research Associates, Cincinnati, Ohio, under NASA Contract NAS3-15558. Specimens taken both parallel and transverse to the sheet rolling direction were creep and stress-rupture tested between 1145 and 1590 K. Additional creep and stress-rupture testing of TD-NiCr sheet, TD-NiCrAl sheet, and IN-853 bar was performed at the Lewis Research Center. All creep and stress-rupture testing was done in accordance with ASTM Specification E139-69. In addition, a few TD-NiCr thermal fatigue and flexural fatigue specimens were examined for evidence of diffusional creep. The methods used for these fatigue tests are described in references 18 and 19. Table II summarizes all test conditions evaluated.

Upon completion of testing, a piece of test section approximately 2 centimeters long from each sample was mounted for examination. In all cases, the mounted section was parallel to the gage length; thus, for sheet specimens, the directionality of the mounted section and test specimen are the same. The mounted specimens were metallographically polished through 0.05-micrometer Al_2O_3 and then electrolytically stain etched with either (1) a chromic acid mixture (100 cm^3 H_2O, 10 cm^3 H_2SO_4, and 2 g chromic acid)

TABLE II. - TEST CONDITIONS EVALUATED

Material	Heat	Rolling direction and test direction	Type of test	Temperature		Stress, MN/m^2	Duration, hr	Elongation, percent
				K	T/T_m			
TD-NiCr	3636	Parallel	Stress rupture	1590	0.95	27.5	45.5	4.1
		Normal		1590	.95	17.0	50.8	12.0
		Parallel		1475	.88	41.5	176.0	1.4
		Normal		1475	.88	24.0	73.0	11.6
		Normal		1475	.88	27.5	483.6	----
		Parallel		1365	.82	73.0	148.0	3.7
		Normal		1365	.82	41.0	377.5	24.0
		Parallel		1255	.75	96.5	186.1	4.3
		Normal		1255	.75	72.5	310.7	7.0
		Parallel		1145	.69	132.0	132.2	2.3
		Normal		1145	.69	107.0	253.1	4.9
	3090	Parallel		1365	.82	41.0	240.0	----
	3637	Normal	Creep	1255	.75	62.0	136.8	.94
	3637	Normal	Creep	1365	.82	48.0	425.5	.4
	3697	Normal	Creep	1255	.75	62.0	136.8	.13
	----	--------	Thermal fatigue	1475	.88	-----	100 1/2-hr cycles	----
	----	Parallel	Flexure fatigue	1470	.88	-----	4344 cycles 24.1 hr	----
TD-NiCrAl	3774	Normal	Creep	1365	.82	31.0	50.0	8.0
IN-853	----	Bar stock	Stress rupture	1310	.82	110.0	[a]1030.0	----

[a]Temperature increased to 1365 K; failed in 18 additional hr.

or (2) buffered aqua regia (two parts by volume aqua regia and one part glycerine) at 3 to 5 volts.

It has been previously shown (ref. 20) that these etchants delineate ThO_2-free regions from ThO_2-dispersed regions. To confirm the ThO_2 distribution, several tested specimens were examined with an electron microprobe. Concentration profiles were determined by standard point-to-point techniques with Cr K_α, Ni K_α, and Th M_α characteristic radiation being continuously monitored and recorded. The microprobe was operated at 15 kilovolts and 50 nanoamperes specimen current with a beam size approximately 2 micrometers in diameter. In addition, several tested specimens were examined by electron replication metallography to determine the thoria distribution.

RESULTS

TD-NiCr Sheet

Stress rupture tested specimens. - Post-test metallographic examination of stress rupture tested 0.051-centimeter-thick TD-NiCr sheet (heat 3636 tested at various stress levels between 1145 and 1590 K in air both parallel and normal to the sheet rolling direction) revealed the presence of whitish-gray bands, voids, and in some cases, intergranular oxides along certain grain boundaries. Representative photomicrographs are presented in figure 3. In all cases, the regions shown in figure 3 are some distance from

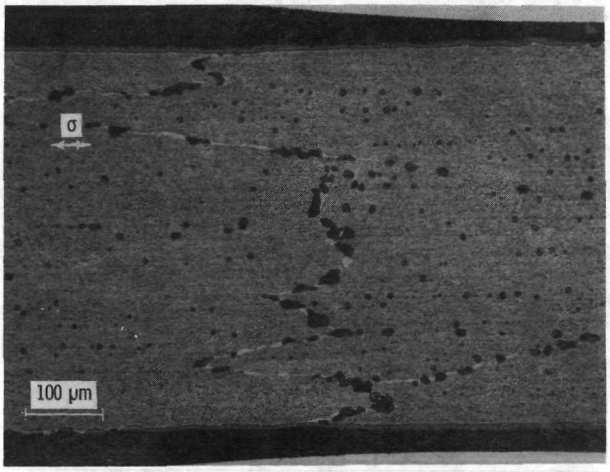

(a) Tested at 1590 K and 27.5 MN/m^2 for 45.5 hours. Percent elongation, 4.1. (Parallel.)

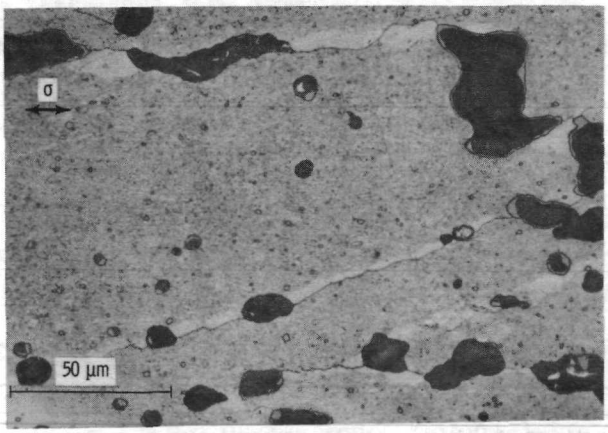

(b) Tested at 1590 K and 27.5 MN/m^2 for 50.8 hours. Percent elongation, 12.0. (Normal.)

Figure 3. - Effects of stress rupture testing on microstructure of 0.051-centimeter-thick TD-NiCr sheet (heat 3636). Electrolytically etched with chromic acid mixture.

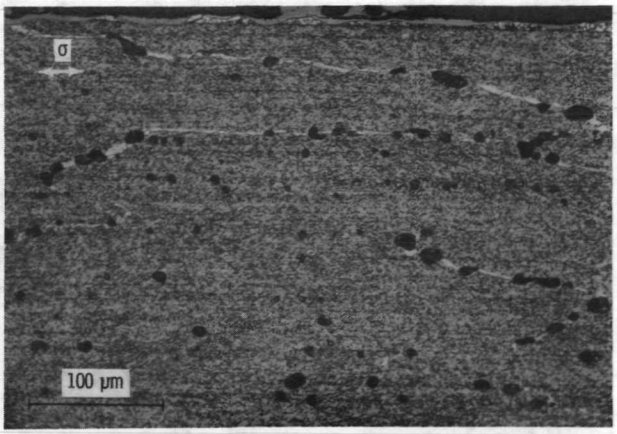

(c) Tested at 1475 K and 41.5 MN/m^2 for 176 hours. Percent elongation, 1.4. (Parallel.)

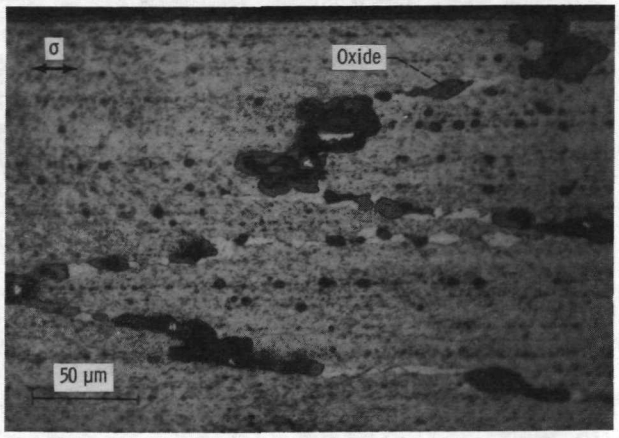

(d) Tested at 1365 K and 73 MN/m^2 for 148 hours. Percent elongation, 3.7. (Parallel.)

Figure 3. - Continued.

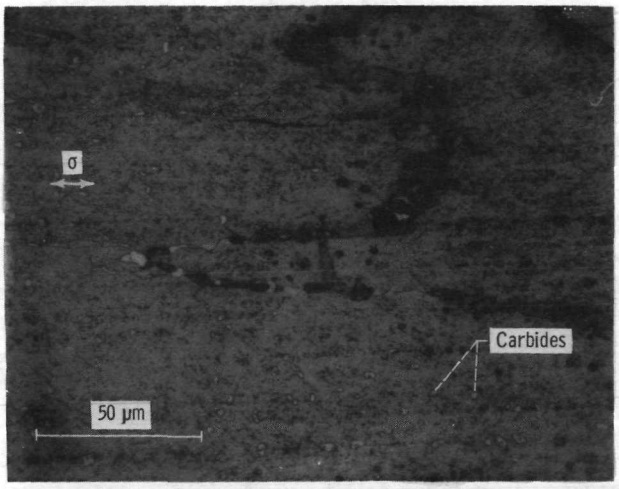

(e) Tested at 1255 K and 96.5 MN/m^2 for 186.1 hours. Percent elongation, 4.3. (Parallel.)

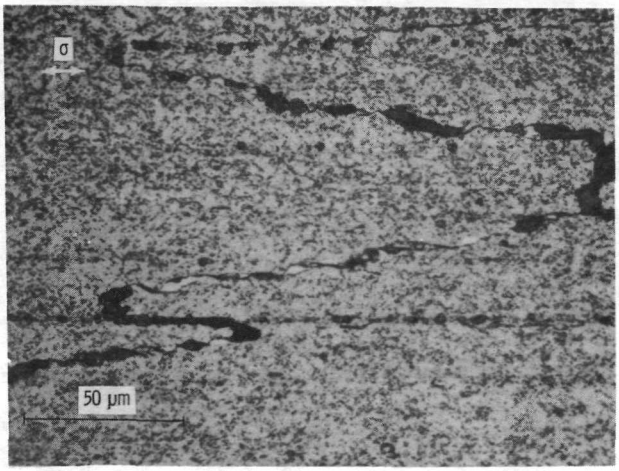

(f) Tested at 1145 K and 132 MN/m^2 for 132.2 hours. Percent elongation, 2.3. (Parallel.)

Figure 3. - Concluded.

the fracture zones. In the course of this examination, the following observations were made as typical of most of the specimens examined:

(1) The whitish-gray bands contain grain boundaries (e.g., fig. 3(b)).

(2) The whitish-gray bands generally interconnect voids (cracks) and/or intergranular oxides (e.g., fig. 3(d)).

(3) The size of the cracks is greatest for bands which are perpendicular to the stress axis (e.g., fig. 3(a)).

(4) The whitish-gray bands formed during testing at the lower temperatures, 1255 and 1145 K, are narrow (e.g., figs. 3(e) and (f)).

(5) Precipitates, probably chromium carbides, were seen after testing at 1255 and 1145 K (e.g., fig. 3(e)).

(6) Neither whitish-gray bands, cracks, nor intergranular oxides were seen at every grain boundary.

(7) At all test temperatures examined, the post-test microstructure was the same for samples tested either normal or parallel to the sheet rolling direction.

Of primary importance is the observation of the whitish-gray bands in these specimens. To distinguish the effects of stress and temperature on the formation of these bands, several similar specimens were heat treated (without external stresses) in air and then metallographically examined. Typical microstructures of these specimens are shown in figure 4. The whitish-gray bands were not observed in these specimens. Thus, formation of these bands appears to depend on both stress and temperature.

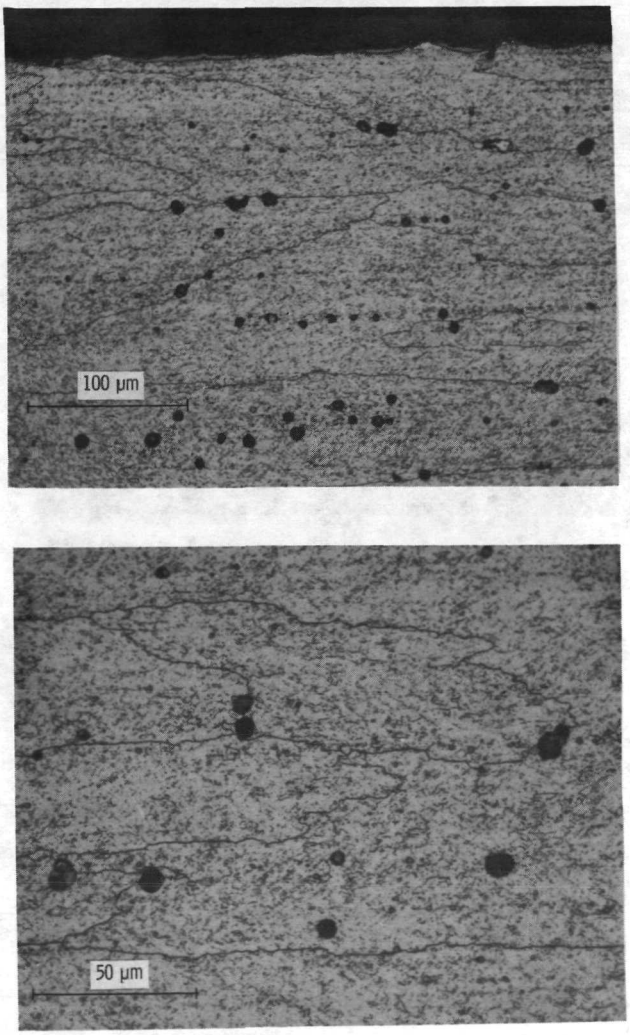

Figure 4. - Effect of annealing on microstructure of 0.051-centimeter-thick TD-NiCr sheet (heat 3636). Mounted section parallel for rolling direction; annealed 50 hours at 1590 K in air. Electrolytically etched with chromic acid mixture.

Previous studies (ref. 20) of diffusion in thoriated Ni-Cr alloys had shown similar whitish-gray regions to be thoria-free. To determine if the bands formed in these stress-rupture tested specimens were thoria-free, several specimens were examined with the aid of the electron microprobe. Appropriate chromium and thorium intensity profiles and photomicrographs are shown in figures 5 and 6. These data indicate that the whitish-gray bands are thoria-free and that the chromium concentrations in the band and surrounding matrix are similar. To further examine the thoria distribution, several tested specimens were studied by electron replication metallography. This technique also indicated that the bands were thoria-free. A typical thoria-free band is shown in figure 7. Note that a grain boundary is visible in this band.

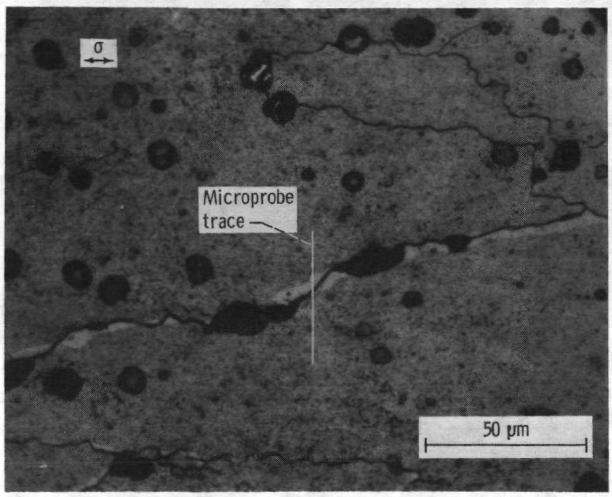

(a) Photomicrograph of region corresponding to trace 1. Electrolytically etched with chromic acid mixture.

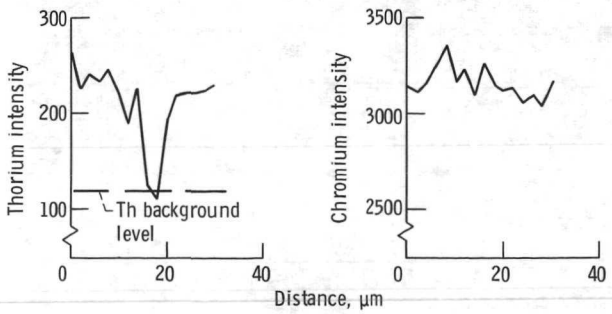

(b) Thorium profile for trace 1.

(c) Chromium profile for trace 1.

Figure 5. - Evidence of thoria-free zones in a 0.051-centimeter-thick TD-NiCr sheet (heat 3636) specimen after stress-rupture testing at 1590 K and 17 MN/m^2. Life, 50.8 hours; elongation, 12 percent. (Normal.)

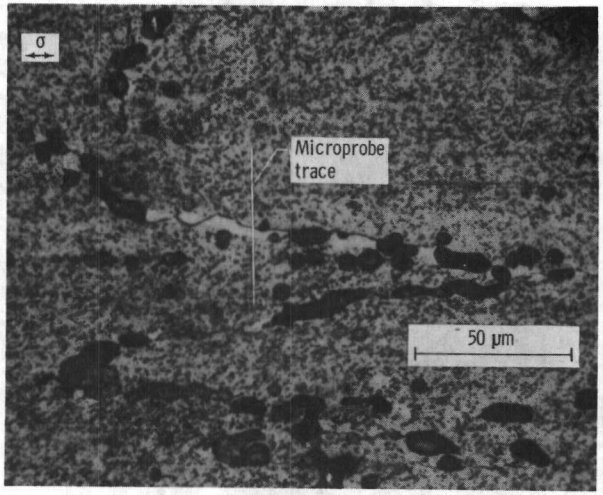

(a) Photomicrograph of region corresponding to trace 6. Electrolytically etched with chromic acid mixture.

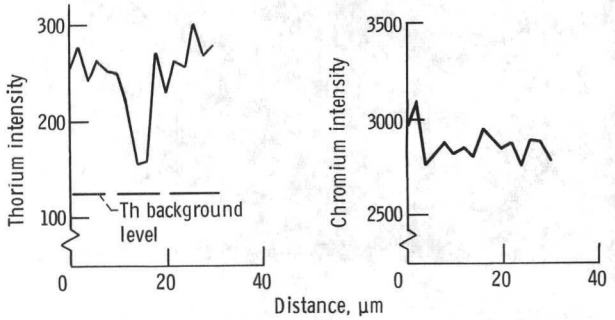

(b) Thorium profile for trace 6.

(c) Chromium profile for trace 6.

Figure 6. - Evidence of thoria-free zones in a 0.051-centimeter-thick TD-NiCr sheet (heat 3636) specimen after stress-rupture testing at 1365 K and 73 MN/m^2. Life, 148 hours; elongation, 3.7 percent. (Parallel.)

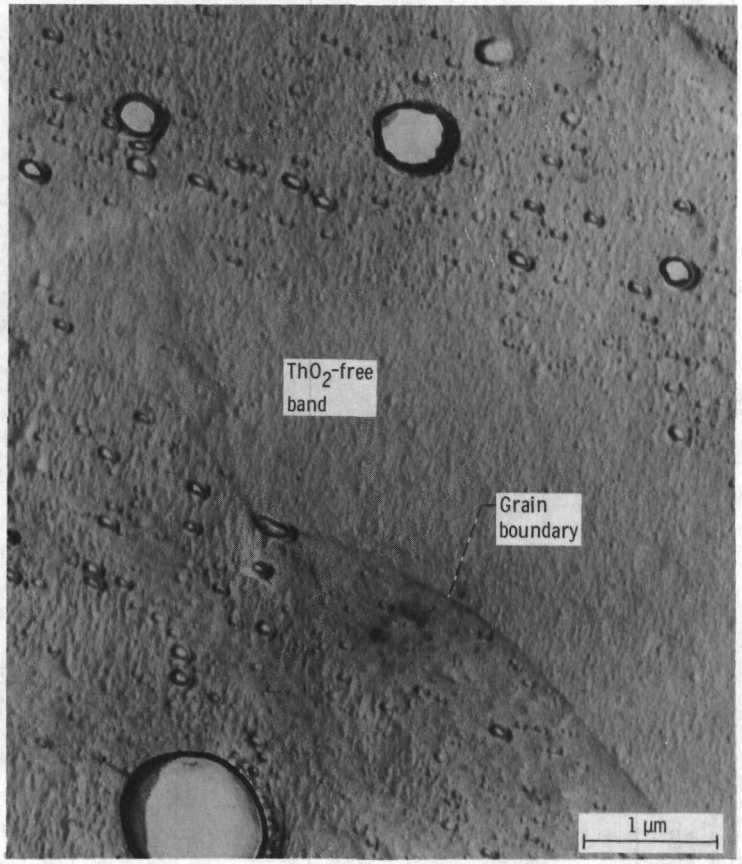

Figure 7. - Electron replica photomicrograph of thoria-free band in a TD-NiCr sheet (heat 3636) specimen tested at 1590 K and 27.5 MN/m^2. Life, 45.5 hours; elongation, 4.1 percent. (Parallel.)

The microstructure of thicker (0.16 cm) TD-NiCr sheet was also examined after stress rupture testing to assess the effect, if any, of sheet thickness on these observations. As was the case for thin TD-NiCr sheet, ThO_2-free regions, voids, and intergranular oxides were observed. Typical photomicrographs are shown in figure 8. Thus, the creep deformation process in TD-NiCr sheet appears to be independent of thickness in the range of 0.051 to 0.16 centimeter.

Examination of a few TD-NiCr specimens tested in vacuum also revealed the presence of both ThO_2-free bands and voids. For comparative specimens tested either in air or vacuum under similar conditions (1365 K and 31 MN/m^2), the vacuum tested specimens exhibited much shorter lives than the air-tested specimens; this is in agreement with the results of Wilcox et al. (ref. 14). Because of the shorter testing time in

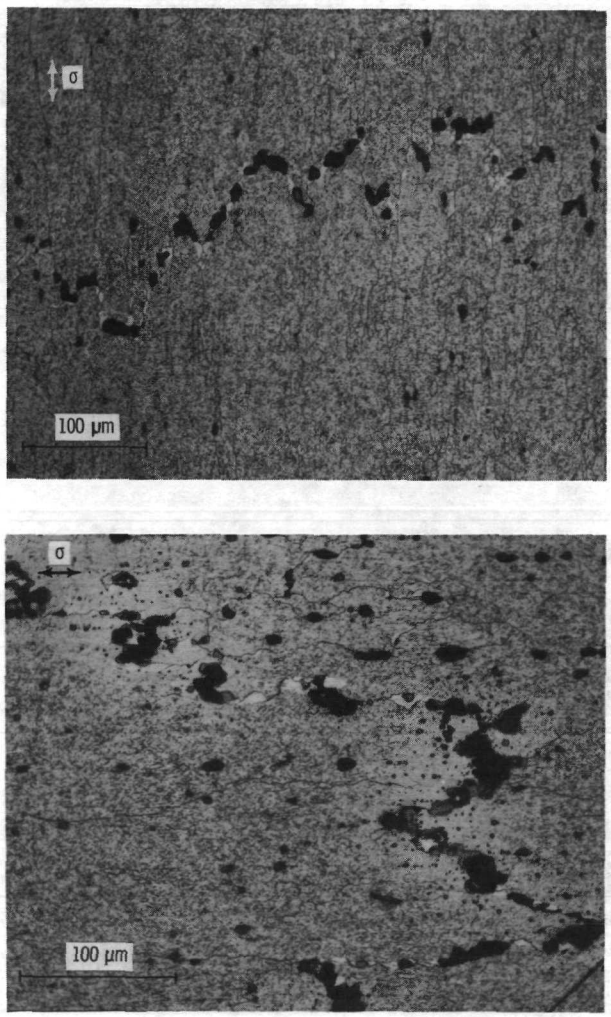

Figure 8. - Effect of stress rupture testing on 0.16-centimeter-thick TD-NiCr sheet (heat 3090). Tested at 1365 K and 41 MN/m^2 for 240 hours. (Parallel.) Electrolytically etched with chromic acid mixture.

the vacuum tests, the ThO_2-free bands observed in these specimens were quite narrow.

Creep tested specimens. - Since stress rupture tests usually result in large deformation (>1 percent), creep tested specimens were also examined for the formation of thoria-free bands. Typical photomicrographs of several specimens are shown in figure 9. As shown, thoria-free bands and voids were observed - even with as little as 0.13 percent creep deformation.

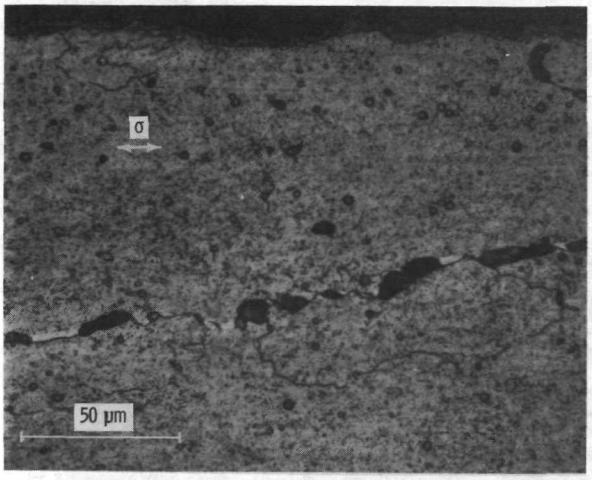

(a) Tested at 1255 K and 62 MN/m^2 for 136.8 hours. Percent creep, 0.94. (Heat 3637.)

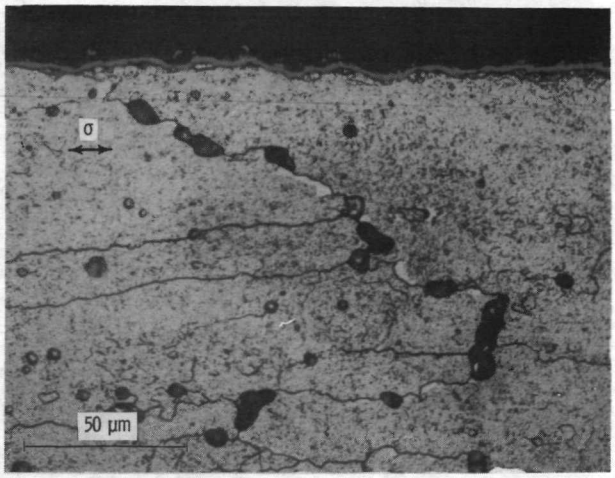

(b) Tested at 1365 K and 48 MN/m^2 for 425.5 hours. Percent creep, 0.4. (Heat 3637.)

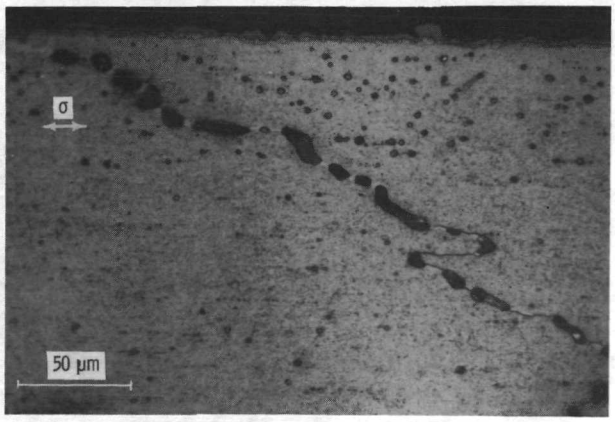

(c) Tested at 1255 K and 62 MN/m^2 for 136.8 hours. Percent creep, 0.13. (Heat 3697.)

Figure 9. - Effects of creep testing on 0.025-centimeter-thick TD-NiCr sheet. (Normal.) Electrolytically etched with chromic acid mixture.

Fatigue-tested specimens. - Photomicrographs of TD-NiCr specimens which had been subjected to thermal fatigue and flexural fatigue testing at 1470 K are shown in figure 10. Evidence of ThO_2-free regions also can be seen in these photomicrographs. In the thermal fatigue specimens, the ThO_2-free bands tended to be parallel to the compressive stresses caused by thermal expansion. (This observation is consistent with models of diffusional creep under an applied compressive stress.) In the flexural fatigue specimens, ThO_2-free bands formed in regions under tension or compression (opposite sheet surfaces), but thoria-free bands did not form near the zero stress axis

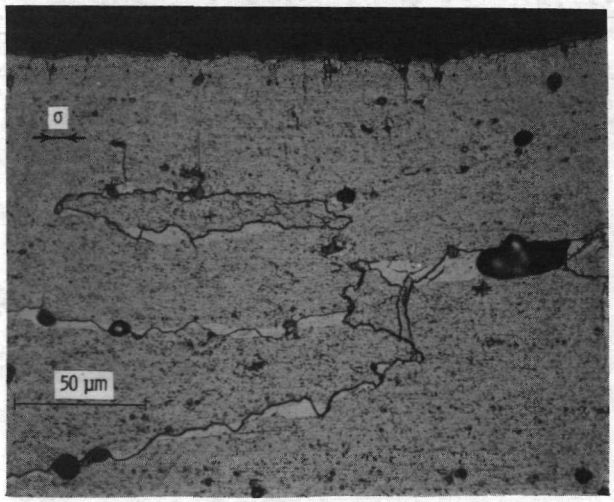

(a) Thermal fatigue: 100 1/2-hour cycles at 1470 K in 1300-N/m^2 air. (From ref. 18.)

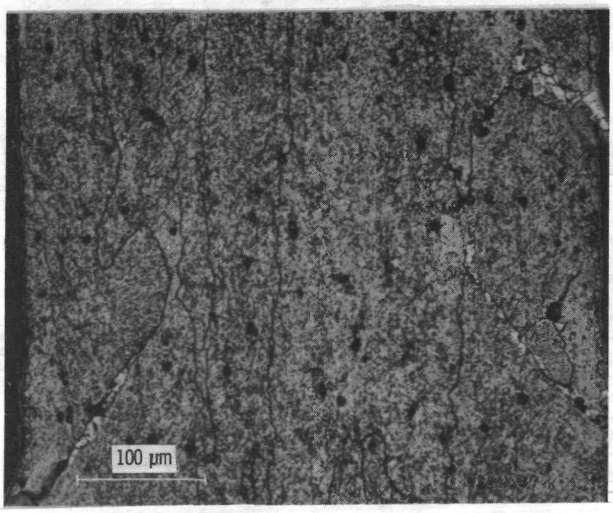

(b) Flexural fatigue: 4344 cycles in 24.1 hours at 1475 K in air. (From ref. 19.)

Figure 10. - Effects of high temperature fatigue tests on microstructure of 0.05-centimeter-thick TD-NiCr sheet. Electrolytically etched with chromic acid mixture.

(center of the sheet). Generally, the effects of high temperature deformation processes in these fatigue specimens appear to be similar to those observed in the stress-rupture and creep tests.

TD-NiCrAl and IN-853 Alloys

Creep tested TD-NiCrAl sheet. - TD-NiCrAl is a modified form of TD-NiCr containing about 3 to 5 percent aluminum for improved oxidation resistance (ref. 17). Experimental lots of this alloy have been evaluated by creep testing at 1365 K. Metallographic examination of tested specimens indicated that this alloy also forms ThO_2-free zones, pores, and intergranular oxides. Typical photomicrographs are shown in figure 11.

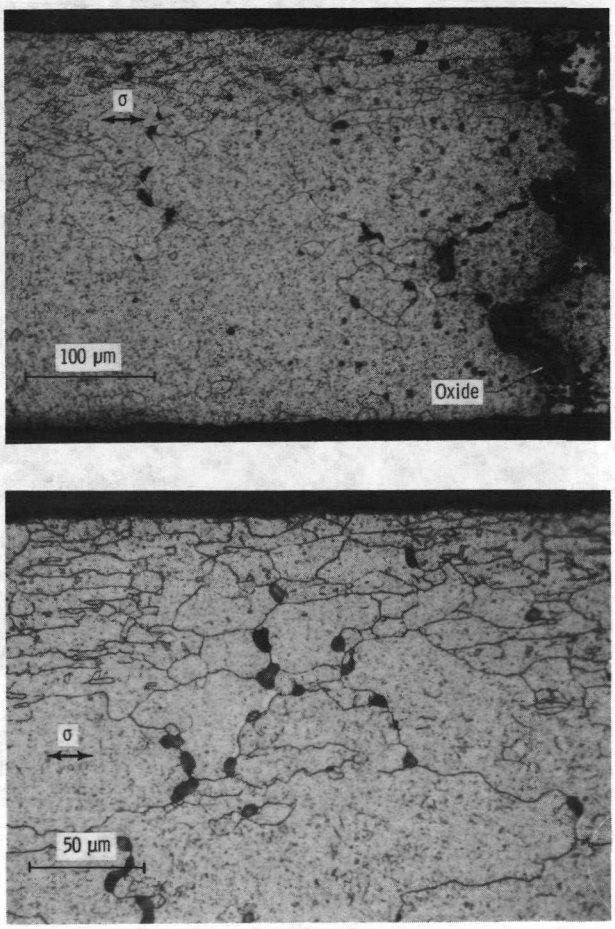

Figure 11. - Effects of creep testing on microstructure of 0.025-centimeter thick TD-NiCrAl sheet (heat 3774) at 1365 K and 31 MN/m^2 for 50 hours; percent elongation, 8; fractured on cooling. Electrolytically etched with chromic acid.

Stress rupture tested IN-853 bar. - The alloy IN-853 is a recently developed alloy designed to have γ' strengthening at intermediate temperatures and to have inert oxide (Y_2O_3) dispersion strengthening at high temperatures. The microstructure of IN-853 bar consists of coarse cylindrical grains of irregular cross section, approximately 0.1 centimeter in diameter by approximately 0.5 centimeter in length. Typical photomicrographs of a stress-rupture-tested specimen are shown in figure 12. If we assume that the buffered aqua regia etchant reveals Y_2O_3-free zones as it reveals ThO_2-free zones, the microstructure of crept IN-853 is similar to that of TD-NiCr with the exception that intergranular oxides were not observed in this alloy.

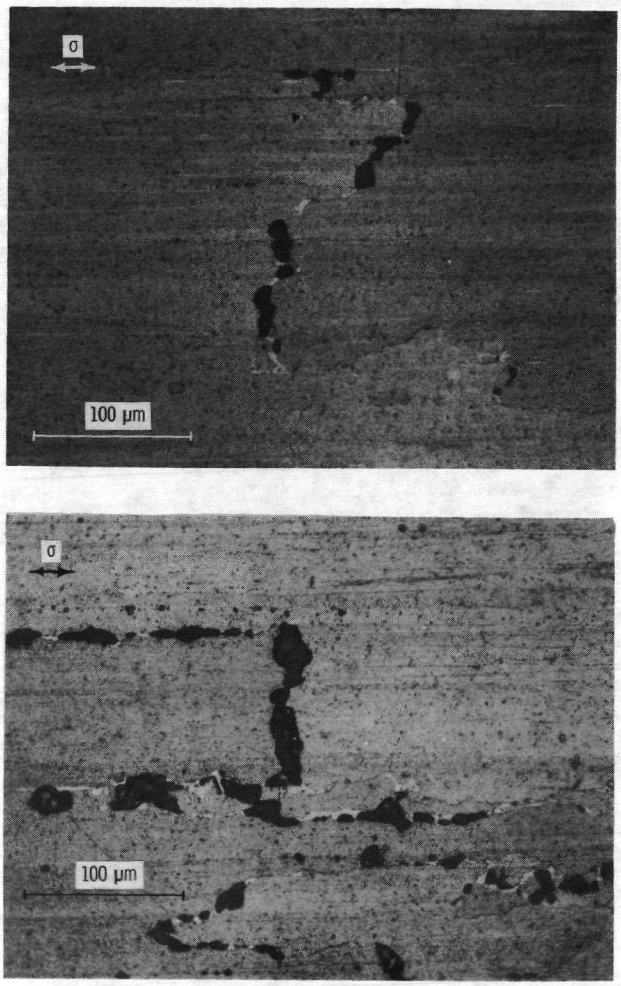

Figure 12. - Effects of stress rupture testing on microstructure of IN-853 bar. Initially tested at 1310 K and 110 MN/m^2 for 1030 hours, then tested at 1355 K and 110 MN/m^2 for 18 additional hours. Electrolytically etched with buffered aqua regia.

DISCUSSION

TD-NiCr Sheet

From the photomicrographs and concentration profiles of stress rupture tested, creep tested, and fatigue tested TD-NiCr, it is evident that the initial ThO_2 particle dispersion at grain boundaries is disrupted. Thus, we concluded that the high temperature, slow strain rate deformation of TD-NiCr is, at least partially, controlled by a diffusional creep mechanism where grain boundaries acting as vacancy sources become surrounded by ThO_2-free bands. As the dispersoid-free bands grow in thickness, the effectiveness of dispersion strengthening is reduced; and the alloy degrades to a duplex microstructure, where the stronger dispersion-strengthened material is separated by ThO_2-free bands. Further deformation tends to localize in the weaker ThO_2-free material, producing voids which can grow and ultimately lead to cracks and failure.

Apparently, in the TD-NiCr tested in air, the problem of diffusional creep and void formation is compounded by intergranular oxidation in the ThO_2-free regions since the oxidation resistance of Ni-20Cr is much less than that of Ni-20Cr-2ThO_2 (ref. 21). In general, intergranular oxidation should quickly lead to failure. But, in this case, oxidation appears to strengthen the static load bearing capacity of TD-NiCr (ref. 14). However, after examination of several oxidation-strengthened specimens, we found that the room temperature ductility and impact resistance was impaired since the specimens fractured during handling.

The postulated sequence of creep degradation in TD-NiCr is shown schematically in figure 13. The steps are (1) formation of ThO_2-free zones due to diffusional creep, (2) formation of voids (cracks) due to the high stresses in the weaker Ni-20Cr, (3) growth and interconnection of voids to form paths leading to the sheet surfaces, and (4) intergranular oxidation in the ThO_2-free bands starting at voids. The overall effect of such degradation would be continuous reduction of the mechanical properties with increasing creep strain, as is shown in figure 2. Therefore, even though TD-NiCr exhibits good creep and stress rupture strength between 1255 and 1475 K, creep degradation of the microstructure can be quite severe.

The apparent strengthening of TD-NiCr due to intergranular oxidation is of great importance. This effect leads to very long stress rupture lives, but this is coupled with a severely degraded microstructure. Typical photomicrographs of these microstructures are shown in figure 14. Once intergranular oxidation begins, creep of TD-NiCr sheet is probably controlled by the conversion of metal to oxide, which apparently leads to long lives and large elongation values. Thus, one must be extremely careful when using TD-NiCr stress rupture data obtained in air for design purposes. This is particularly important for thin sheet because of the thin cross section. What

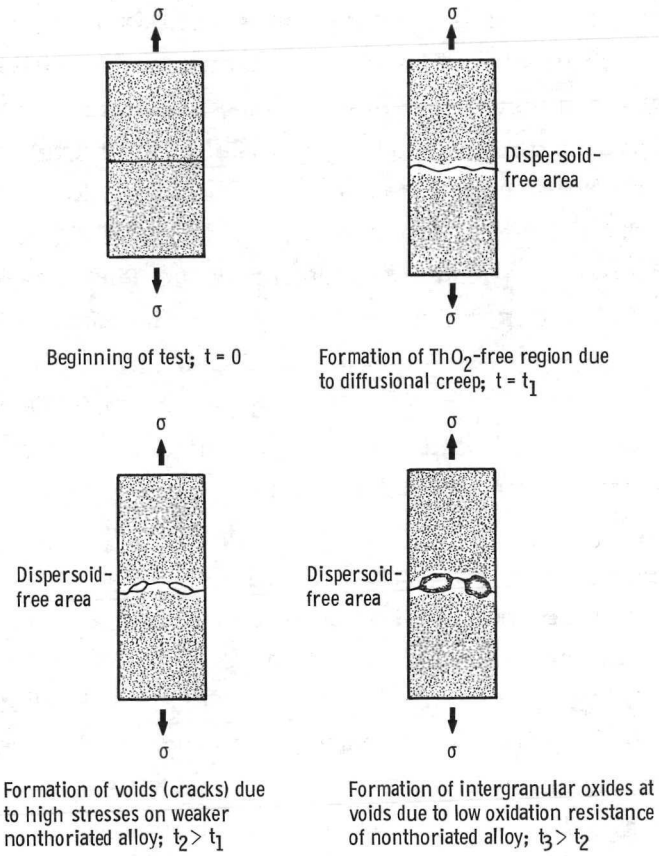

Figure 13. - Schematic representation of degradation of TD-NiCr during creep testing in air.

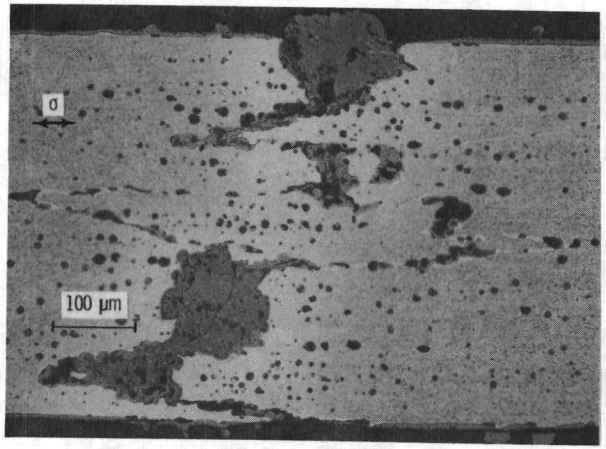

(a) Tested at 1590 K and 27.5 MN/m^2 for 45.5 hours. Percent elongation, 4.1. (Parallel.) (General light staining around oxides due to chromium loss by diffusion to oxide.)

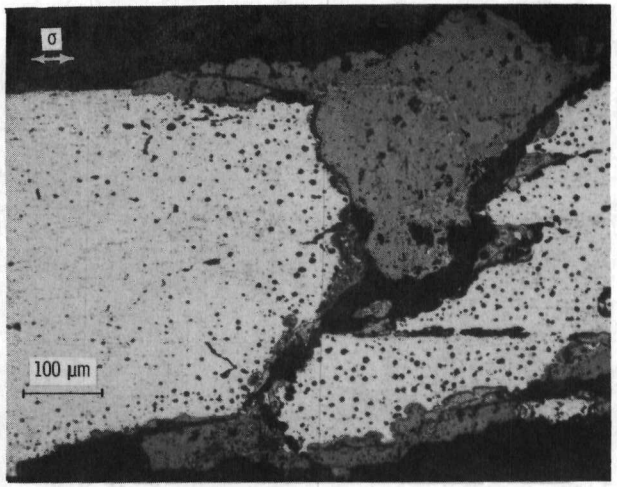

(c) Tested at 1365 K and 41 MN/m^2. Failed on unloading after 377.5 hours. (Normal.) Unetched.

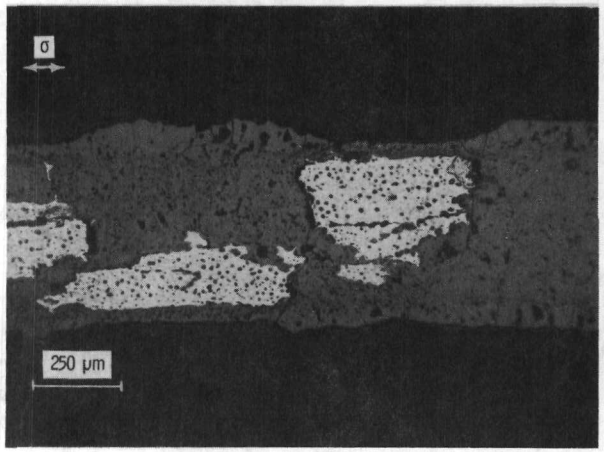

(b) Tested at 1475 K and 27.5 MN/m^2. (Normal.) Failed on unloading after 483.6 hours.

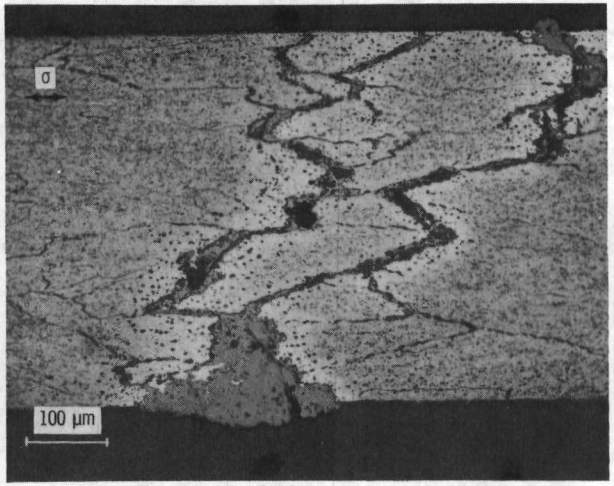

(d) Tested at 1255 K and 72.5 MN/m^2 for 310.7 hours. Percent elongation, 7. (Normal.)

Figure 14. - Massive oxidation in stress rupture tested 0.051-centimeter thick TD-NiCr sheet (heat 3636). Electrolytically etched with chromic acid mixture, unless noted.

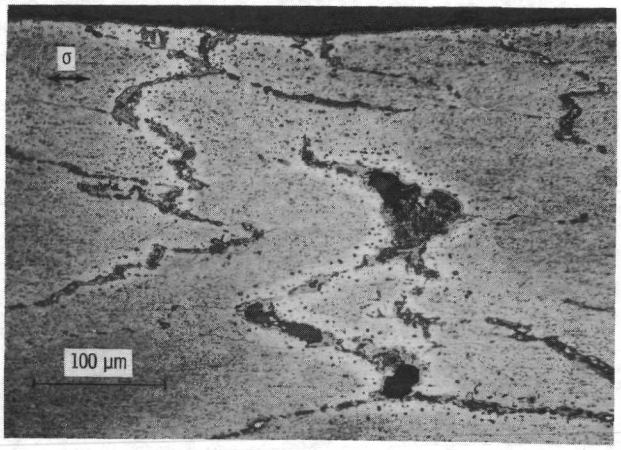

(e) Tested at 1145 K and 107 MN/m^2 for 253.1 hours. Percent elongation, 4.9. (Normal.)

Figure 14. - Concluded.

effects this type of oxidation has on thicker sections of TD-NiCr are not known.

One possible way to avoid these intergranular oxidation effects on TD-NiCr would be to apply a protective coating on the surfaces. During subsequent high temperature testing, the behavior of the coated TD-NiCr should be similar to that of uncoated material tested either in vacuum or inert atmosphere. Failure should occur through growth and coalescence of the voids formed in the ThO_2-free regions (fig. 13(c)), and the strength of the coated TD-NiCr will be less than that of the uncoated material tested in air (ref. 14).

TD-NiCrAl Sheet

The photomicrographs shown in figure 11 indicate that the effect of creep in TD-NiCrAl is similar to that in TD-NiCr. ThO_2-free bands are formed at grain boundaries which serve as vacancy sources. These bands then act as sites for void formation and apparently for intergranular oxidation. This oxidation is probably the result of interconnecting porosity which leads to the sheet surfaces. In addition, it appears that TD-NiCrAl is also strengthened by intergranular oxidation (fig. 11) in the same manner as TD-NiCr. This would lead to long stress rupture lives coupled with a degraded microstructure.

IN-853 Bar

IN-853 also appears to undergo diffusional creep since Y_2O_3-free bands and voids in these bands were seen after stress-rupture testing (fig. 12). It should be noted that

intergranular oxidation was not observed in this alloy. Apparently, there is no intergranular oxidation in the dispersoid-free zones of IN-853 because the large, elongated grain structure prevents the formation of interconnecting porosity. On the other hand, TD-NiCr and TD-NiCrAl sheet have a much smaller grain structure (pancake-shaped grains approximately 50 μm in thickness by 150 μm in length) which allows interconnecting porosity leading to the surfaces. Therefore, IN-853 bar would probably not be affected by the oxidation strengthening exhibited by TD-NiCr and TD-NiCrAl.

Creep Model

Proposed model for diffusional creep. - The critical step in creep degradation of dispersion-strengthened Ni-base alloys appears to be the formation of dispersion-free regions by diffusional creep. With the assumption that volume diffusion is the controlling step, there are two simple models in the literature predicting the diffusional creep rate $\dot{\epsilon}$:

$$\dot{\epsilon} = \frac{\alpha \sigma D \nu}{R^2 kT} \tag{1}$$

and

$$\dot{\epsilon} = \frac{\alpha D \nu}{R^2 kT} (\sigma - \sigma_0) \tag{2}$$

Equation (1) describes the creep rate of a Newtonian viscous solid (Nabarro-Herring model, refs. 4 and 5), where α is a constant ($2 \leq \alpha \leq 25$), σ is the applied stress, D is the volume diffusion coefficient, ν is the volume per atom, 2R is the average grain diameter, k is Boltzmann's constant, and T is the absolute temperature. Equation (2) is a modified form which describes the creep rate in a Bingham solid (ref. 22), where σ_0 is the threshold stress needed to initiate creep. That is, in order for creep to occur in a Bingham solid, the applied stress must exceed the threshold stress.

Inherent in the derivation of the preceding equations is the assumption that all grain boundaries are perfect vacancy sinks or sources once the threshold stress is exceeded ($\sigma_0 = 0$ for eq. (1)); thus, dispersoid-free bands should be formed at every possible boundary. As noted in the section RESULTS, ThO_2-free bands were not seen at every possible grain boundary after slow strain rate, high temperature testing of TD-NiCr. Therefore, neither equation (1) nor equation (2) adequately describes diffusional creep in TD-NiCr. However, equation (2) could be modified to fit the experimental observations if it is postulated that a range of threshold stresses exists. Thus, an increasing

number of vacancy sinks and sources would be activated as the applied stress is raised.

In general, a strain rate equation with variable threshold stresses will be complicated; however, a rather simple formulation can be developed on the basis of two assumptions: (1) the material in question can be partitioned into columns where each column is 1 grain width in diameter with length L (see fig. 15), and (2) all columns experience the same strain. These assumptions simply divide the material into elements which experience equal creep strain. This division is possible since the specimen geometry cannot allow different creep strains in each element. Note that no assumption is made about the specific sites of creep in each element. Any accommodation necessary between neighboring columns will be accomplished by grain boundary sliding, which is an integral part of diffusional creep (ref. 23).

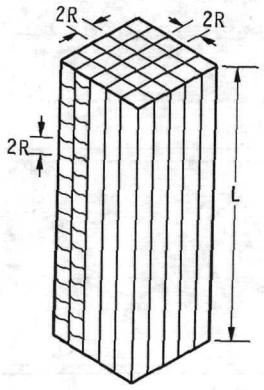

Figure 15. - Schematic model for postulation of variable threshold stresses for creep. Material partitioned into columns of length L and of approximate diameter 2R. All columns composed of equiaxed grains approximately 2R in diameter.

To calculate the strain rate for any column of grains, one must sum all the individual creep extensions $\dot{\ell}$ (distance/unit time) at each active creep site in the column and divide this total by the column length. With reference to the Nabarro-Herring creep model (eq. (1)), the creep extension at any boundary transverse to the tensile stress is

$$\dot{\ell} = \frac{2\alpha D\nu\sigma}{RkT} \tag{3}$$

Modification of equation (3) to include the concept of a variable threshold stress yields

$$\dot{\ell} = \frac{2\alpha D\nu}{RkT}\left(\sigma - \sigma_0^i\right) \tag{4}$$

where $\dot{l}_i$ is the creep extension at the vacancy source i and σ_0^i is the threshold stress for site i. Thus, the strain rate for any column of grains is

$$\dot{\epsilon} = \frac{1}{L} \sum_{i=1}^{m} \dot{l}_i = \frac{2\alpha D\nu}{LRkT} \sum_{i=1}^{m} \left(\sigma - \sigma_0^i\right) \tag{5}$$

where L is the column length (gage length) and m is the number of active sites in the column. In order for creep to occur at site i, the applied stress must exceed σ_0^i. Each σ_0^i depends on the particle distribution in the boundary, the temperature, and probably many other microscopic variables (ref. 22). The maximum number of possible creep sites is limited both by the column length L and the average grain diameter 2R such that $m \leq L/2R$. Obviously, the stress and temperature dependencies of equation (5) are complicated since the number of active sites increases with increasing temperature and applied stress.

If grain boundary diffusion is the controlling step, then an equation similar to equation (5) can be developed from the Coble model (ref. 6):

$$\dot{\epsilon} = \frac{2\beta\nu}{LRkT} \frac{\delta D_B}{R} \sum_{i=1}^{m} \left(\sigma - \sigma_0^i\right) \tag{6}$$

where β is a constant ($\beta \approx 50$), δ is the thickness of the grain boundary, and D_B is the grain boundary diffusion coefficient. Comparison of equations (5) and (6) reveals that diffusional creep will occur primarily by atom migration along grain boundaries when

$$\frac{D_B}{D} > \frac{\alpha}{\beta} \frac{R}{\delta} \tag{7}$$

Comparison with general creep model. - In general, the steady state creep rate $\dot{\epsilon}_s$ in dispersion-strengthened metals has been described by

$$\dot{\epsilon}_s \propto \sigma^n \exp\left(-\frac{Q_c}{kT}\right) \tag{8}$$

With this approach, unusually high stress exponents n and/or creep activation energies Q_c have been reported (refs. 12 to 15). If either equation (5) or equation (6) is the rate-controlling process and if equation (8) is used to describe the creep rate, high values for n and/or Q_c can result. For example, at a constant temperature, small changes in

the applied stress can produce many more active creep sites; this would produce a high stress dependency. At a constant stress, changes in the test temperature would produce a large change in the creep rate if the threshold stresses were temperature sensitive; this would result in a high creep activation energy.

Application of proposed model. - The creep rates calculated from either equations (1), (2), (5), or (6) inherently assume that the general microstructure of the creep specimens remains unchanged throughout the test (i.e., voids or intergranular oxides are not formed). But the previously presented photomicrographs indicate that this is not the case for TD-NiCr, even for creep deformations as low at 0.13 percent. While void formation should increase the diffusional creep rate, intergranular oxidation could have the opposite effect. In addition, it should be noted that both equations (5) and (6) describe the diffusional creep in an equiaxed material with grain diameter 2R. But most dispersion-strengthened Ni-base alloys generally have nonequiaxed grains; for example, TD-NiCr sheet has pancake-shaped grains where the grain aspect ratio (length-thickness ratio) is approximately 3. In general, increasing the grain aspect ratio would reduce the diffusional creep rate since the maximum number of creep sites m would be reduced.

While equations (5) and (6) do not describe the creep rate for the entire creep test, they do describe the creep rate during the most important stage of creep - while dispersoid-free regions are beginning to form (i.e., before void formation and/or intergranular oxidation). Thus, these equations can be useful to determine methods of reducing the effects of diffusional creep. To reduce the creep rate, ideally one should increase the threshold stresses σ_0^i, but this may be difficult since the factors which control the threshold stress are not well known. Furthermore, it will be difficult to ensure that every grain boundary has a high threshold stress. Alternatively, increasing the grain size and/or decreasing the number of possible active creep sites (e.g., increasing the grain aspect ratio of the alloy) should reduce the creep rate. However, to eliminate any possibility of forming dispersoid-free regions, all grain boundaries must be removed.

GENERAL REMARKS

The dispersion-strengthened alloy TD-NiCr was developed to have good creep strength at high temperatures ($T/T_M > 0.7$). While it apparently has such characteristics on the basis of conventional stress-rupture and creep properties (ref. 17), examination of the post-test microstructure reveals that ThO_2-free regions, voids, and in some cases, intergranular oxides have been formed. This loss in alloy integrity appears to be initiated by diffusional creep which forms ThO_2-free regions. These regions then provide sites for void formation and possible internal oxidation. The apparent high

temperature strength of TD-NiCr tested in air results in part from the strengthening effects of oxidation. Unfortunately, material so strengthened exhibits little impact resistance and vastly reduced low-temperature strength and ductility. To prevent this loss of alloy integrity, the allowable creep deformation must be kept small (<0.1 percent).

The results of slow strain rate, high temperature testing of TD-NiCrAl, IN-853, and Mg-ZrH_2 alloys (refs. 7 to 10) and γ' strengthened Ni-base alloys (refs. 11 and 12) reveal that the formation of dispersoid-free regions is not unique to TD-NiCr or even to dispersion-strengthened alloys. Apparently, diffusional creep is an important mechanism whenever normal dislocation mechanisms are not activated or dislocation movement is blocked.

CONCLUSIONS

The following conclusions are drawn on the basis of metallographic examination of TD-NiCr specimens (and a few specimens of TD-NiCrAl and IN-853) after they were tested in air at slow strain rates and high temperature:

1. Diffusional creep appears to be an active mechanism in the deformation of TD-NiCr, and it may be characteristic of all dispersion-strengthened alloys.

2. Diffusional creep caused degradation of TD-NiCr through formation of a duplex microstructure with dispersoid-free zones near selective grain boundaries. Since the dispersoid-free zones are generally weaker than the matrix, void (crack) formation occurs preferentially in these zones.

3. Creep degradation appears to be compounded in air-tested TD-NiCr by preferential oxidation of the thoria-free zones. This intergranular oxidation results in an apparent strengthening of the material but has detrimental effects on the ductility and impact resistance.

Lewis Research Center,
National Aeronautics and Space Administration,
Cleveland, Ohio, September 7, 1972,
502-21.

APPENDIX - DIFFUSIONAL CREEP

Creep in polycrystalline materials normally involves dislocation multiplication and motion; however, creep can take place without dislocation mechanisms being activated. At low stress and high temperature, creep can occur simply through the creation and motion of vacancies. This process is termed "diffusional creep" (refs. 4 to 6). Essentially, an applied tensile stress reduces the energy required to produce vacancies at grain boundaries which tend to be perpendicular to the tensile stress. This results in a higher concentration of vacancies at these boundaries than at boundaries parallel to the stress. Because of the concentration difference, vacancies tend to diffuse from sources (grain boundaries normal to the applied tensile stress) to sinks (grain boundaries parallel to the applied tensile stress). This behavior is shown schematically in figure 16.

The net and continuous flow of vacancies from sources to sinks produces diffusional creep. The vacancy flow is counterbalanced by an equal flow of atoms (fig. 17). In a simple single-phase polycrystalline material, the mass flow due to diffusional creep would not produce any microstructural changes other than elongating the grains in the direction of the applied tensile stress. However, in polycrystalline material which contains a uniform distribution of inert second-phase particles, the mass flow due to diffusional creep would result in particle-free regions in the vicinity of the grain boundaries which act as vacancy sources. During creep, a mass of material necessary to compensate for the net production of vacancies would be absorbed at these boundaries. This mass would form particle-free regions since the mass must bypass the particles in order to reach the grain boundaries (see fig. 1, p. 2). Therefore, diffusional creep in a dispersion (or precipitation)-strengthened alloy results in a duplex microstructure, where particle-free regions separate particle-containing regions.

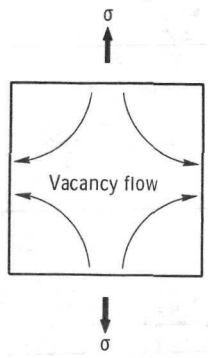

Figure 16. - Schematic representation of vacancy flow in grain subjected to applied tensile stress.

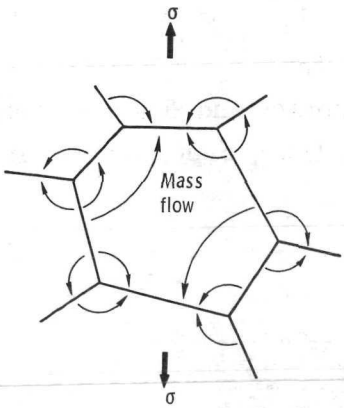

Figure 17. - Schematic representation of mass flow in polycrystalline grain subjected to tensile stress. (After Herring, ref. 5.)

REFERENCES

1. Ansell, G. S.: The Mechanism of Dispersion Strengthening. A review. Oxide Dispersion Strengthening. George S. Ansell, Thomas D. Cooper, and T. V. Lenel, eds., Gordon and Breach Science Publ., 1968, pp. 61-141.

2. Ashby, M. F.: The Mechanical Effects of a Dispersion of a Second Phase. Second International Conference on the Strength of Metals and Alloys. Vol. 2, ASM, 1970, pp. 505-541.

3. Wilcox, B. A.; Clauer, A. H.; and Hutchinson, W. B.: Structural Stability and Mechanical Behavior of Thermalmechanically Processed Dispersion-Strengthened Nickel Alloys. NASA CR-72832. March, 1971.

4. Nabarro, F. R. N.: Deformation of Crystals by the Motion of Single Ions. Report on the Conference on Strength of Solids. Physical Society, London, 1948, pp. 75-90.

5. Herring, Conyers: Diffusional Viscosity of a Polycrystalline Solid. J. Appl. Phys., vol. 21, no. 5, May 1950, pp. 437-445.

6. Coble, R. L.: A Model for Boundary Diffusion Controlled Creep in Polycrystalline Materials. J. Appl. Phys., vol. 34, no. 6, June 1963, pp. 1679-1682.

7. Squires, R. L.; Weiner, R. T.; and Phillips, M.: Grain-Boundary Denuded Zones in a Magnesium-1/2 wt % Zirconium Alloy. J. Nucl. Mat., vol. 8, no. 1, Jan./Feb. 1963, pp. 77-80.

8. Karim, Anwar-ul; Holt, David L.; and Backofen, Walter A.: Diffusional Creep and Superplasticity in a Mg-6Zn-0.5 Zr Alloy. Trans. AIME, vol. 245, no. 5, May 1969, pp. 1131-1132.

9. Karim, Anwar-ul; Holt, David L.; and Backofen, Walter A.: Diffusional Flow in a Hydrided Mg-0.5 wt pct Zr Alloy. Trans. AIME, vol. 245, no. 11, Nov. 1969, pp. 2421-2424.

10. Rainey, P. E.; and Holt, D. L.: An Observation by Transmission Electron Microscopy of Diffusional Creep in a Magnesium Alloy. Met. Trans., vol. 2, no. 11, Nov. 1971, pp. 3238-3239.

11. Decker, R. F.; and Freeman, J. W.: The Mechanism of Beneficial Effects of Boron and Zirconium on Creep Properties of a Complex Heat-Resistant Alloy. Trans. AIME, vol. 218, no. 2, Apr. 1960, pp. 277-285.

12. Gibbons, T. B.: The Influence of Diffusional Creep on Precipitate-Free Zone Formation in Ni-20% Cr-Base Alloys. Met. Sci. J., vol. 6, no. 1, Jan. 1972, pp. 13-16.

13. Wilcox, B. A.; and Clauer, A. H.: Creep of Thoriated Nickel Above and Below 0.5 T_m. Trans. AIME, vol. 236, no. 4, Apr. 1966, pp. 570-580.

14. Wilcox, B. A.; Clauer, A. H.; and McCain, W. S.: Creep and Creep Fracture of a Ni-20Cr-2ThO_2 Alloy. Trans. AIME, vol. 239, no. 11, Nov. 1967, pp. 1791-1796.

15. Wilcox, B. A.; and Clauer, A. H.: Creep of Dispersion-Strengthened Nickel-Chromium Alloys. Met. Sci. J., vol. 3, 1969, pp. 26-33.

16. Benjamin, J. S.; and Cairns, R. L.: Elevated Temperature Mechanical Properties of a Dispersion-Strengthened Superalloy. Modern Developments in Powder Metallurgy. Vol. 5. H. H. Hausner, ed., Plenum Press, 1971, pp. 47-71.

17. Klinger, L. J.: Development of Dispersion-Strengthened Nickel-Chromium-Thoria Sheet for Space Shuttle Vehicles, Part I. NASA CR-120796, 1972.

18. Sanders, W. A.; and Barrett, C. A.: Oxidation Screening at 1204° C (2200° F) of Candidate Alloys for the Space Shuttle Thermal Protection System. Space Shuttle Materials. SAMPE, 1971, pp. 709-718.

19. Hirschberg, Marvin H.; Spera, David A.; and Klima, Stanley J.: Cyclic Creep and Fatigue of TD-NiCr (Thoria-Dispersion-Strengthened Nickel-Chromium), TD-Ni, and NiCr Sheet at 1200 C. NASA TN D-6649, 1972.

20. Whittenberger, John D.: Diffusion in Thoriated and Nonthoriated Nickel and Nickel-Chromium Alloys at 1260° C. NASA TN D-6797, 1972.

21. Giggins, C. S.; and Pettit, F. S.: The Oxidation of TD-NiC (Ni-20Cr-2 vol pct ThO_2) Between 900° and 1200° C. Met. Trans., vol. 2, no. 4, Apr. 1971, pp. 1071-1078.

22. Ashby, M. F.: On Interface-Reaction Control of Nabarro-Herring Creep and Sintering. Scripta Met., vol. 3, no. 11, 1969, pp. 837-842.

23. Raj, R.; and Ashby, M. F.: On Grain Boundary Sliding and Diffusional Creep. Met. Trans., vol. 2, no. 4, Apr. 1971, pp. 1113-1127.

NASA-Langley, 1972 —— 17 E-7080

NATIONAL AERONAUTICS AND SPACE ADMISTRATION
WASHINGTON, D.C. 20546

OFFICIAL BUSINESS
PENALTY FOR PRIVATE USE $300

FIRST CLASS MAIL

POSTAGE AND FEES PAID
NATIONAL AERONAUTICS AND
SPACE ADMINISTRATION

U.S.MAIL

NASA 451

POSTMASTER: If Undeliverable (Section 158 Postal Manual) Do Not Return

"The aeronautical and space activities of the United States shall be conducted so as to contribute . . . to the expansion of human knowledge of phenomena in the atmosphere and space. The Administration shall provide for the widest practicable and appropriate dissemination of information concerning its activities and the results thereof."

—NATIONAL AERONAUTICS AND SPACE ACT OF 1958

NASA SCIENTIFIC AND TECHNICAL PUBLICATIONS

TECHNICAL REPORTS: Scientific and technical information considered important, complete, and a lasting contribution to existing knowledge.

TECHNICAL NOTES: Information less broad in scope but nevertheless of importance as a contribution to existing knowledge.

TECHNICAL MEMORANDUMS: Information receiving limited distribution because of preliminary data, security classification, or other reasons.

CONTRACTOR REPORTS: Scientific and technical information generated under a NASA contract or grant and considered an important contribution to existing knowledge.

TECHNICAL TRANSLATIONS: Information published in a foreign language considered to merit NASA distribution in English.

SPECIAL PUBLICATIONS: Information derived from or of value to NASA activities. Publications include conference proceedings, monographs, data compilations, handbooks, sourcebooks, and special bibliographies.

TECHNOLOGY UTILIZATION PUBLICATIONS: Information on technology used by NASA that may be of particular interest in commercial and other non-aerospace applications. Publications include Tech Briefs, Technology Utilization Reports and Technology Surveys.

Details on the availability of these publications may be obtained from:

SCIENTIFIC AND TECHNICAL INFORMATION OFFICE

NATIONAL AERONAUTICS AND SPACE ADMINISTRATION

Washington, D.C. 20546